Materials Research Express

PAPER

Influence of temperature on the creep behaviour by macroindentation of Cocos nucifera shells and Canarium schweinfurthii cores (bio-shellnut wastes in Cameroon)

Bernard Morino Ganou Koungang[1,2], **Dieunedort Ndapeu**[1], **Jerôme Tchoufang Tchuindjang**[3], **Bernard Wenga Ntcheping**[3], **Gilbert Tchemou**[1], **Sophie Bistac**[4], **Ebénézer Njeugna**[1] and **Luc Courard**[2]

[1] LAboratoire de Mécanique et Matériaux Adaptés (LAMMA), University of Douala, 1872 Douala, Cameroun
[2] Urban and Environmental Engineering (UEE), Laboratoire des Matériaux de Construction (LMC), Université de Liège (ULiège), Allée de la Découverte, 9, 4000 Liège, Belgique
[3] Aerospace and Mechanical Engineering (AME), Metallic Materials Science Unit (MMS), University of Liege (ULiège), Allée de la Découverte, 9, 4000 Liege, Belgium
[4] Chemical and Physical Chemistry of Polymer (CPCP), Laboratoire de photochimie et d'ingénierie macromoléculaires (LPIM), 68100 Mulhouse, France

E-mail: morinoganou@yahoo.fr

Keywords: Cocos nucifera, Canarium schweinfurthii, macroindentation, creep, Rheology, Ashby classification

OPEN ACCESS

RECEIVED
25 August 2020

REVISED
23 September 2020

ACCEPTED FOR PUBLICATION
6 October 2020

PUBLISHED
14 October 2020

Abstract

The aim of this study was to show how temperature modifies the mechanical characteristics of the Cocos nucifera (CN) shells and the Canarium schweinfurthii (CS) cores. The test consisted in performing an instrumented macroindentation on prismatic specimens in an adiabatic chamber; the indentation carried out according to four temperature ranges (30 °C, 50 °C, 70 °C, 90 °C). The Oliver and Pharr method is used for the analysis of mechanical parameters in indentation: reduced Young's modulus, hardness, creep coefficient. These parameters have enabled to estimate indirect characteristics such as toughness and ultimate mechanical stress to be obtained. The creep data are simulated to have the rheological model to these materials by considering the statistical criteria. As a global observation, when the temperature increases, the mechanical parameters decrease; although CN is more sensitive to the temperature gradient than CS, these 2 materials show performances that allow them to be classified as engineering polymer materials according to the Ashby diagram.

1. Introduction

Biomaterials are a class of materials comprising biofibres, biopolymers and bio-composites, the main components of which come from agriculture or the plant world, as products or wastes [1–5]. These materials have experienced a boom in recent years, regarding many issues such as reduction of plastic pollution, recycling, stiffness, lightweight, low cost, etc. People are seeking to replace synthetic materials that have a negative impact on the environment and life, causing harmful effects on land, sea and air [1, 2, 6], by natural materials that are biodegradable [2, 6, 7].

The field of use of biomaterials is large, including construction industry [1, 4, 5, 8–10], thermal, sound and electrical insulated components [1, 4–6, 11–15], but also as parts for wear resistance [1] or those exhibiting improved impact strength [1, 3, 6, 11, 12, 16, 17]. Many other applications related to biocomposites have also be found in the automotive field [1, 5, 11].

The development of new materials [18–20] requires the determination of their mechanical properties [21, 22] when considering various scales starting from the macro to nano scale. Natural biomaterials are among these new materials [23, 24], and due to their availability they are increasingly used in industry as secondary resources that can replace or supplement primary resources [25–27]: *Cocos nucifera* (CN) shells and *Canarium schweinfurthii* (CS) cores are among these bioresources which are available as waste in Cameroon, with an estimated volume around 2,000 tons [28].

CN and CS biomaterials can be used alone, such as timber for construction and structural purposes [13, 29–32]. But their most extensive use is achieved with composites, in the forms of reinforcements within a matrix of either polymer [1, 2, 5–7, 12, 14, 15, 29, 33–36], ceramic [1, 5], metallic [1, 5, 37], or hybrid type [5, 7, 8, 11, 16, 17].

In the case of CN, several distinct parts of the coconut have already been studied [1, 2, 6, 11, 13, 15, 30, 31, 33, 34, 36, 38]. CN fibres are reported to exhibit the highest toughness amongst natural fibres [10]. The CN shell, including the one transformed into powder, has been added to various matrix while considering distinct preparations [2, 4, 5, 33, 36, 37]. In addition, other parts of the CN plant are sometimes used, such as leaves [11, 36], trunk or stems [13, 30, 31], and this occurs either as bearing materials or as composites.

When these natural materials are in the form of fibres, surface preparation [1, 6, 7, 9, 12, 14, 34, 36] and/or physical or chemical pre-treatments [8–10, 16, 17, 34] are needed in order to achieve the best interface with the matrix and/or an improvement within the strength of the fibres.

In the case of CS, technical applications as a composite material lead to characterization approaches that are similar to those already mentioned for CN, with the enhancement of the effect of density, the water absorption rate, and friction properties [29, 35]. Recent work has focused on producing brake linings by combining CS fillers and palm kernel fiber with urea formaldehyde resin. He was interested in the effect of input size and proportions on composite density and dynamic friction coefficient [39]. Standard mechanical characterization can also be carried out for parts of CS when they are in their natural state, such as strength and stiffness [32] or strength and mobility for nuts, the humidity level being an important parameter in the latter case [40].

Biomaterials exhibit a hierarchical structure [3, 38, 41–43] with complex morphologies [1, 3, 30, 38, 41–43], which makes it difficult to achieve complete characterization.

However, characterization is necessary to better understand the material's behaviour, so as to be to identify or to extend the field of applications, which choice is set depending on the achieved properties. Such an approach is highlighted by works from Schmier *et al* [41] and Gludovatz *et al* [38], who both succeed in identifying the mechanisms of crack initiation and toughening related to the anisotropic channel structure, by establishing the morphological parameters of the hierarchical structure of the CN endocarp. Such results can lay the basis for transferring those properties into biomimetic technical applications [41]. Similarly, a very recent study [42] allows establishing a 3D model of the natural and structured composite material constituted by coconut, in the form of a flat structure with coconut-inspired microchannels. This new approach of numerical simulation allows understanding the crashworthiness of coconuts.

When used as composites, characterization tests for natural materials are quite easy to perform, such as tensile, compression, flexural, etc [1–4, 6, 8, 11, 12, 14–17, 35, 36]. Thermophysical properties of composites can be determined with an equal ease [2, 4, 5, 15–17]. In addition, the dynamic behaviour in connection with dedicated applications is sometimes studied with composites, especially when impact strength is sought [1, 6, 11, 16, 17]. The way fibres or aggregates have to be prepared prior to their incorporation into composites is also well known from many years, including their surface preparation to achieve a good interface with the matrix [1, 7, 12, 14, 33, 36].

For natural materials, the most common mechanical tests are done under static (traction, compression, flexural, etc) or dynamic modes (toughness fracture), either on a single fiber or set of fibers, or on the shell [1, 6, 7, 11, 13, 30, 31, 38, 43], all these features being prompt to exhibit different orientations and a variable age [38]. Thermophysical properties, density as well as water absorption of the fibers or aggregates can also be determined [13, 30, 31, 35, 43].

Several characterization techniques exist [44, 45], including indentation [46] which presents an ideal compromise in relation to the stresses that are applied to the studied material.

Characterization by indentation allows several parameters to be determined at the same time: hardness, Young's modulus, and creep [6, 7, 11, 12]. However, as reported by Flores-Johnson *et al* [3], who determine the hardness of *acrocomia mexicana* fruit shell, such a technique is seldom used for biomaterials characterization. The same observation can be made for creep, which is not often considered for such materials.

The use of these materials is carried out under various conditions, taking into account environmental criteria such as temperature, humidity or acidity, which strongly influence the parameters of the exposed materials [47, 48].

In what follows, the indentation technique will be used to determine the hardness and Young's modulus on both CN and CS biomaterials. In addition, the creep behavior of both materials will be discussed as a function of temperature set at 30, 50, 70 and 90 °C respectively, based on the same indentation tests.

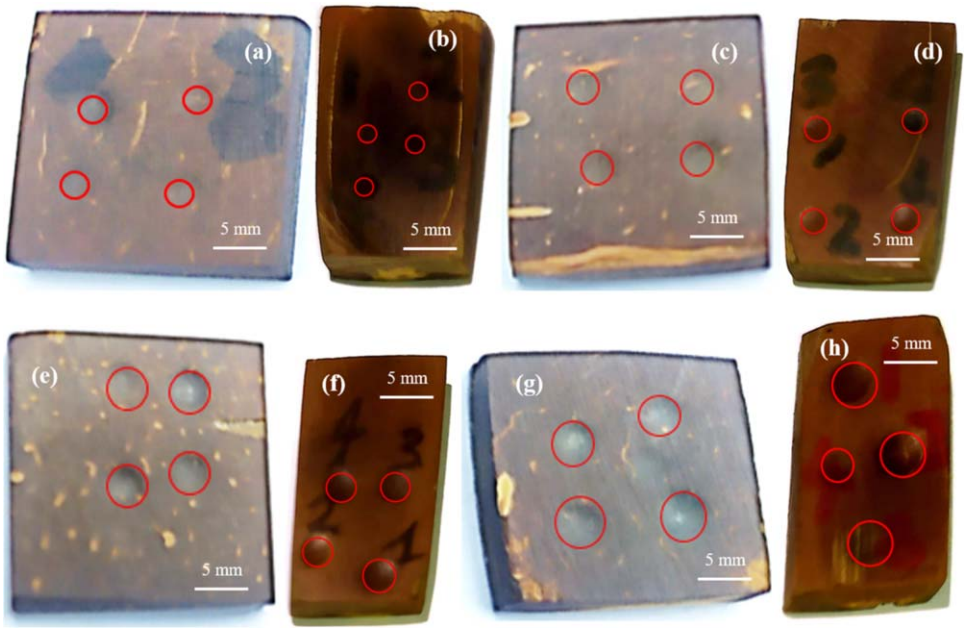

Figure 1. Some sample with indent marks: (a) CN at 30 °C, (a) CS at 30 °C, (c) CN at 50 °C, (d) CS at 50 °C, (e) CN at 70 °C, (f) CS at 70 °C, (g) CN at 90 °C, (h) CS at 90 °C.

2. Materials and methods

2.1. Materials

CS and CN are collected as waste in the public squares of the city of Douala in Cameroon. The cleaning by washing with water of the internal and external surfaces has made it possible to eliminate impurities of the following types: pulp, sludge, sand and fibers. The $10 \times 20 \times 3\ mm^3$ for CS and $10 \times 10 \times 3\ mm^3$ for CN [49] samples (figure 1) were obtained by sawing the shell portions and polishing the faces of this portion.

2.2. 2.2 Methods

The mechanical characterization in this case is carried out at variable temperature but using an adiabatic heating module to maintain a given temperature value around the test sample.

The equipment used by Njeugna, *et al* [49] was modified by adapting the heating module (figure 2).

The experiments are carried out at four temperatures (30 °C, 50 °C, 70 °C, 90 °C) while using *a* spherical indenter of diameter Φ6 mm.

These temperatures are chosen to remain below the glass temperature (Tg) of polymer materials [50–52] (Tg ϵ [100–130] °C). At a given isotherm and for a progressive increase of the load (from 0 up to the maximum load of 500N over a constant incremental step of 50 N), the displacement of the indenter penetrating the specimen is recorded by a $1/1000^{e}$ precision digital sensor. The load-displacement characteristic graph (figure 3(a)) is obtained by combined reading of the sensor displacement display and the corresponding load value. The test is quasi-static but fast enough to avoid creep effects during loading.

When the maximum load is reached and maintained, creep data is recorded over a period of one hour. After creep (figure 3(b)), this is followed by a progressive unloading of each placed mass, during which the data corresponding to the removal of the indenter are also recorded.

The analysis of the indentation tests is based on the hypothesis of an elastoplastic load rise, followed by a purely elastic unloading (figure 4) As far as the analysis and evaluation of the load—unloading curves resulting from the collection of our data is concerned, it has been carried out in several clearly defined steps using the method of Oliver and Pharr [53] expressed by the equation (1).

$$P = P_m\left(\frac{h - h_f}{h_m - h_f}\right)^m. \tag{1}$$

Where P is the force; P_m is the maximum force applied; h is the indentation depth at any time; h_f is the final indentation depth at discharge; h_m is the maximum indentation depth at P_m; m is a constant determined by means of a least squares method and is a function of the geometry of the indenter: for a spherical indenter such as in this study $m = 1$ [54–56].

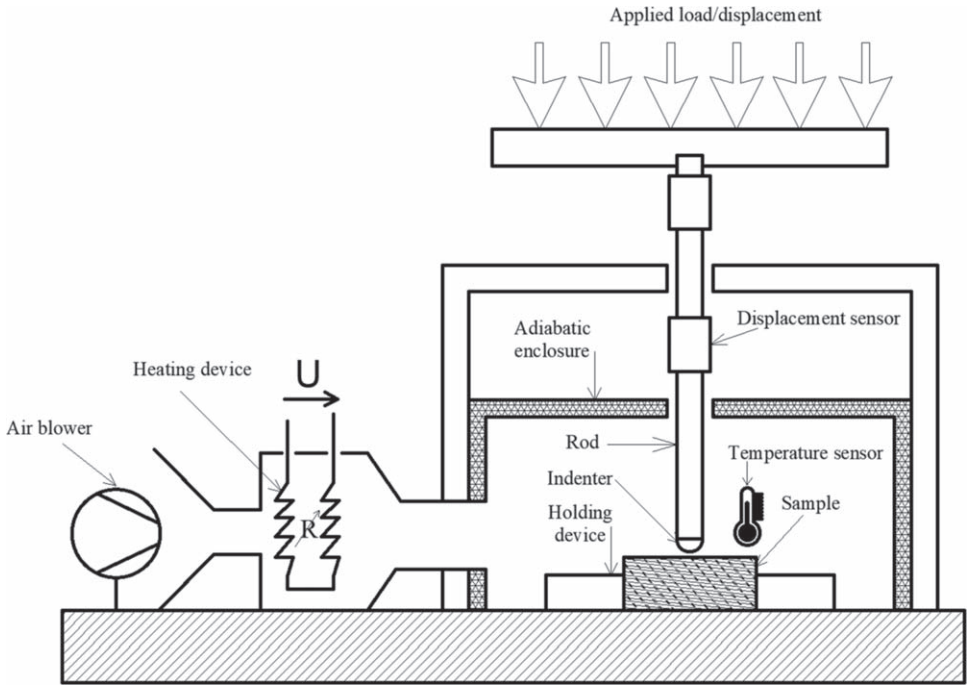

Figure 2. Test device.

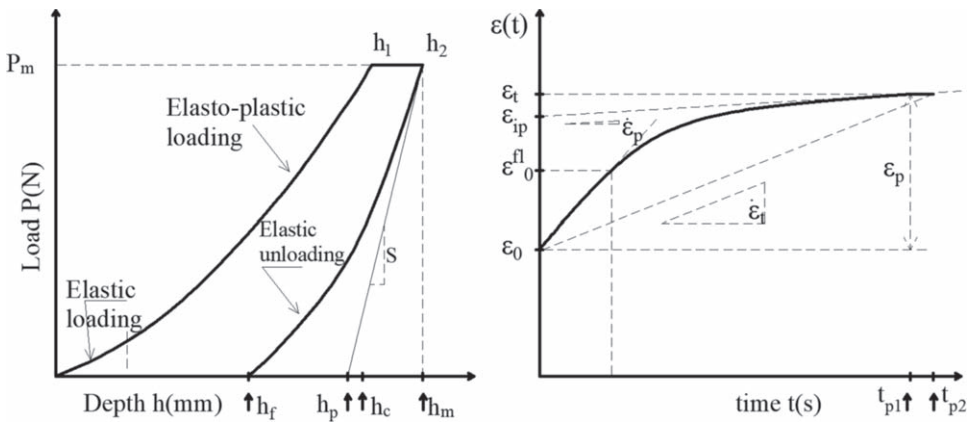

Figure 3. Model curves: (a) indentation; (b) creep.

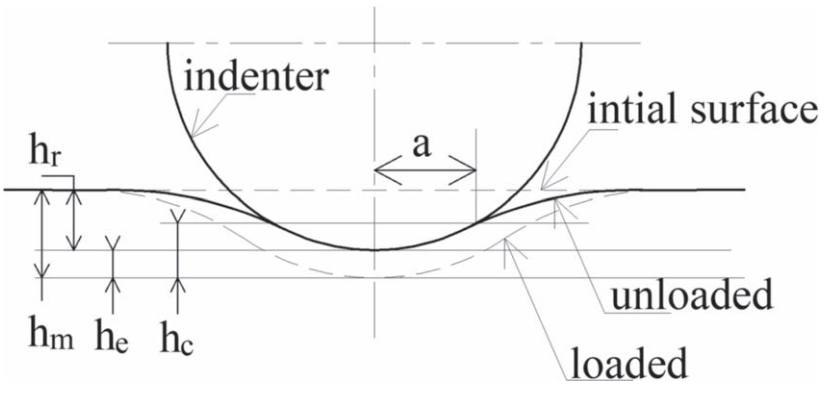

Figure 4. Description of the spherical indentation analysis.

2.2.1. Reduced young's modulus

The determination of Young's modulus is based on the assumption that during the unloading curve the removal of the tip is accompanied by a spring back due to the elasticity of the material. Thus the slope of the unloading curve provides a measure Young's modulus [57–59]. The method is based on the recovery theory of Hertz [60]. It provides for the modelling of the unloading slope with a function that relates the contact area to the reduced Young's modulus according to the equation (2):

$$E_r = \frac{\sqrt{\pi}}{2}\frac{S}{\sqrt{A_c}}. \tag{2}$$

2.2.2. Hardness

Once the method for the calculation of the contact area is available, it is possible to calculate hardness contact H [58, 61]. This is done using the formula from equation (3) and the contact area A_c.

$$H = \frac{P_{\max}}{\sqrt{A_c}} \tag{3}$$

2.2.3. Creep ratio

C_{IT} denoted indentation creep ratio is defined by the relative change in depth of corresponding penetration, according to equation (4).

$$C_{IT} = \frac{h_2 - h_1}{h_1} x\ 100\% \tag{4}$$

when h_1 and h_2 shown in figure 2(a) are the penetrations recorded at the beginning of creep and at the end of creep. In addition to the usual mechanical properties of hardness and modulus of elasticity, the indentation curve gives access to a lot of other interesting information such as elastic and plastic indentation work by measuring the area under the curve as shown in the figure below.

2.2.4. Creep parameters

With regard to the determination of the rheological model, several models are proposed in the literature. These models are based on the combination of springs and dampers to represent the viscoelastic behavior of a material by its total deformation $\varepsilon(t)$ (equation (5)):

$$\varepsilon(t) = \varepsilon^0 + \varepsilon^P \tag{5}$$

The Boltzmann's superposition principle, applied in the case of linear viscoelasticity, states that the sum of the deformations resulting from each component of the stress input is the same as the deformation resulting from the combined stress input, the total deformation can be expressed (equation (6)) by an integral representation such as:

$$\varepsilon(t) = \sigma_0 D(t) + \int_0^t \Delta D(t-\tau)\frac{d\sigma}{d\tau}d\tau. \tag{6}$$

With $D(t)$ and $\Delta D(t-\tau)$ being respectively the creep compliance at the time t and in the transient phase and σ_0 the constant stress.

For non-linear viscoelasticity, the Schapery model is expressed at constant stress using the description of the irreversibility of thermodynamics for the viscoelastic materials subjected to the external loading in single integral [62, 63].

The total deformation (equation (7)) is expressed by:

$$\varepsilon(t) - \varepsilon_{vp}(t) = g_0\sigma_0 D_0 + g_1 g_2 \Delta D\left(\frac{t}{a_\sigma}\right)\sigma_0. \tag{7}$$

The parameters to be determined in the case of the study in only case of creep of nonlinear viscoelasticity are: g_0 (equation (8)), D_0 (equation (9)). The other g_1, g_2, and a_σ are function of recovery and this study is focused only on the creep. During the various tests considering every isotherm.

2.2.4.1. Initial creep compliance D_0

This parameter is obtained as follows:

$$\varepsilon_0(t) = \varepsilon_0 = g_0\sigma_0 D_0 \text{ where } g_0 = 1 \tag{8}$$

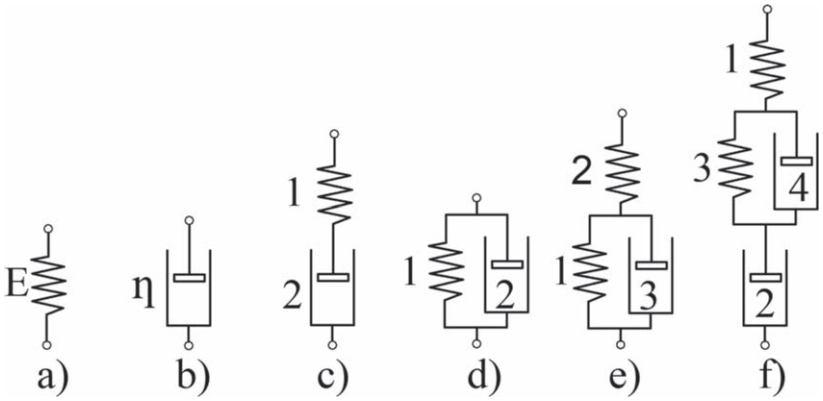

Figure 5. Representation of the rheological models: (a) basic spring model; (b) basic damping model; (c) Maxwell model; (d) Kelvin model; (e) Zener model; (f) Burger model.

Table 1. Rheological model.

Models	Mathematics
Maxwell	$\varepsilon(t) = \frac{\sigma}{E_0} + \frac{\sigma}{\eta_0}t$
Kelvin	$\varepsilon(t) = \frac{\sigma}{E_1}(1 - e^{-\frac{1}{\tau 1}t})$
Zener	$\varepsilon(t) = \frac{\sigma}{E_0} + \frac{\sigma}{E_1}(1 - e^{-\frac{1}{\tau 1}t})$
Burger-4 elements	$\varepsilon(t) = \frac{\sigma}{E_0} + \frac{\sigma}{\eta_0}t + \frac{\sigma}{E_1}(1 - e^{-\frac{\sigma}{\tau 1}t})$

$$\text{By deduction: } D_0 = \frac{\varepsilon_0}{\sigma_0} \tag{9}$$

2.2.4.2. Initial parameter of the non-linearity phenomenon g_0

The parameter g_0 is the one that reflects the non-linearity phenomenon at the beginning of the load when located in the nonlinear viscoelasticity.

It is independent on time and dependent on the load. It is given by the equation (10):

$$\varepsilon^{fl}0 = g_0\sigma_0 D_0 \text{ then } g_0 = \frac{\varepsilon^{fl}0}{\varepsilon_0} \tag{10}$$

$\varepsilon^{fl}0$ and ε_0 are the instantaneous and initial deformations in the linear domain, respectively.

2.2.4.3. Total creep velocity $\dot{\varepsilon}_t$

This parameter is obtained by equation (11).

$$\dot{\varepsilon}_t = \frac{\varepsilon_P}{t_{P2}} = \frac{\varepsilon_t - \varepsilon_0}{t_{P2}} \tag{11}$$

2.2.4.4. Plastic creep velocity $\dot{\varepsilon}_p$

This parameter is obtained by equation (12).

$$\dot{\varepsilon}_p = \frac{\varepsilon_t - \varepsilon_{ip}}{t_{P1}} \tag{12}$$

2.2.5. Rheological model

Several models are obtained by combining the basic elements: spring and damper.

The usual models (figure 5) [64] are listed in table 1. These expressions will be used to test the numerical data obtained during creep acquisition. This in order to know the model that best describes the phenomenon of indentation creep for CN and CS materials.

2.2.6. Density

The test sample is introduced into the cell of the helium pycnometer (Micrometrics 1305). This equipment uses a gas at 140–170 kPa (helium, nitrogen). It is preferably Helium for a best performance, as Helium is stable with all materials. Density was numerically evaluated by (equation (13)).

$$\rho = \frac{m}{v} \tag{13}$$

2.2.7. Toughness

Toughness is assessed by analytical calculation (equation (14)). In general, the mechanical stress of a material can be correlated to the hardness of a material. The relationship between the average pressure under the indenter, the modulus, the yield strength of Young and the hardening behaviors were established. The toughness T of sufficiently hard materials can be obtained using equation (14) as described by Chai, *et al* [65].

$$T = \frac{P_{\max}}{9.3a^{1.5}} \tag{14}$$

The parameter a can easily be identified in figure (3). It is calculated knowing the depth h_c.

2.2.8. Ultimate strength

Since 1945, Bishop, *et al* [8] have suggested that the pressure distribution under an indenter can be approximated by that of a spherical or cylindrical cavity. Relationships between mean pressure under the indenter, yield strength, Young's modulus and strain-hardening behaviour have been established. For plastic solids with perfect elasticity, the pressure (P) at which the cavity extension depends on the ratio between Young's modulus (E) and yield strength (σ_y) and the Poisson's ratio (ν) according to (equation (15))

$$\frac{P}{\sigma_y} = \frac{2}{3}\left(1 + \ln\frac{E}{3(1-\nu)\sigma_y}\right) \tag{15}$$

Following this idea, an extension of the spherical cavity was carried out by Johnson in the early 1970s [66]. He stressed that the radial placement of the material at the elastoplastic limit must take into account the volume of material displaced by the indenter during indentation. Recently, besides these theoretical analyses, an empirical equation is widely used since 1997, the relation between the hardness H and the elastic limit (equation (16)).

$$\sigma \approx \frac{H}{2} \tag{16}$$

It is therefore proven that hardness and ultimate stress are linked by an approximately linear relationship with factors that would depend on the nature of the material.

Thus, considering the data in the literature for materials (acrocomia [3] and macadamia [67]) of the same nature as those under study (CN and CS), a proportionality factor of 2.73 was correlated linking ultimate stress to hardness to obtain (equation (17)).

$$\text{Then } \sigma \approx \frac{H}{2.73} \tag{17}$$

3. Results and discussion

3.1. Hardness, young's modulus, creep coefficient and toughness

Figure 6 shows the results of macroindentation with a maximum applied normal load of 500 N for temperature isotherms of 30, 50, 70 and 90 °C on CN and CS samples. A significant variation is observed on the measured mechanical properties (reduced modulus of elasticity, hardness and indentation toughness) as a function of temperature. The general trend is the reduction of the above parameters.

There is a higher hardness value for CN and CS than for palm nut shells, hazelnut, and brazil nut (table 2) a reduced young modulus value almost twice as high. On the other hand, for materials of the same type such as acrocomia and macadamia, the values for hardness and young modulus are much higher than those for CN and CS. For the Scheelea sp, when the hardness is higher than the hardness of CN and CS; the Young's modulus is slightly smaller. The microstructure and intergranular arrangement are the main factors influencing these parameters. It is also important to specify the scale of the test (macro, micro or nano), the maturity of the shells, the harvesting environment and the climate of the region are very important in the variations often found. Therefore, conducting an effective comparative analysis means integrating all these factors or reducing them by harvesting products from the same area and of the same age. Basically, the analyses carried out here and there

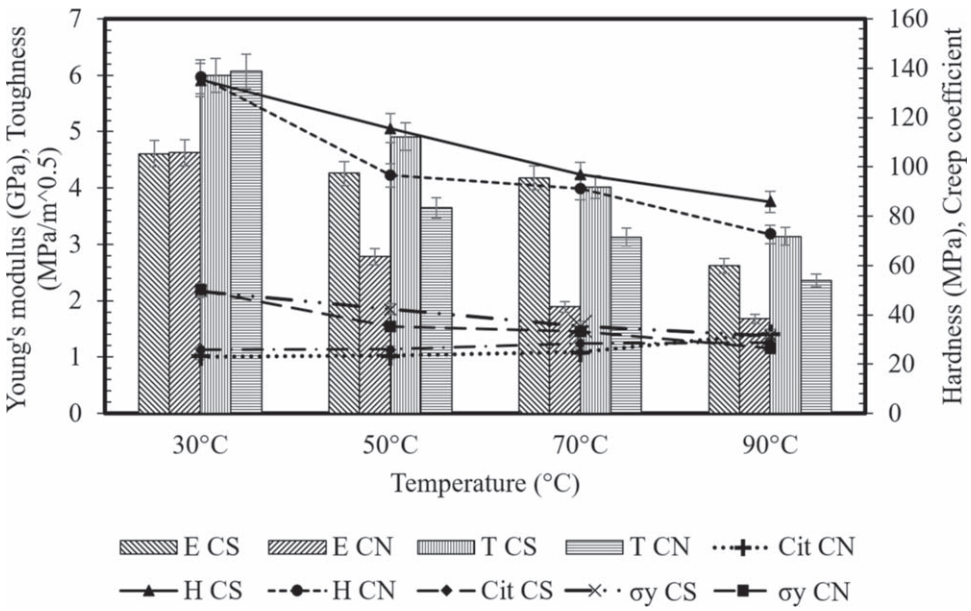

Figure 6. Mechanical results from macroindentation.

just provide a classification range and a criterion to help in the decision making process when selecting materials for specific applications.

3.2. Rheology and creep analysis

Figure 7 shows the creep curve of the CS and CN specimens as a function of temperature. With respect to the evolution of the curves in figure 6, it should be noted that the deformation increases with temperature which is clearly justified in table 3.

By observing the correlation coefficient (R^2) obtained for each rheological model in table 4, the Burger-4 model and the Zener model are showed the best correlation, however, by observing the permanent impressions after discharge and over time, the Burger-4 model is suitable for describing the visco-plasticity of these materials. It shows a correlation trend over all temperature ranges and for both CN and CS. This model adequately describes the phenomenon of indentation creep for these materials. The parameters of the Burger-4 model are given in table 5 and would allow an evaluation of the creep-mechanical parameters describing the visco-plasto-elasticity of this materials.

It appears from figure 6 that CN is more influenced by temperature variation than CS, which is consistent with the density values presented by this work and the SEM microstructures observed by Njeugna, *et al* [52]. Indeed, CN is less dense than CS and CN microstructures show embedded fibers between the grains. Because fibers are more temperature sensitive than the grains of microstructures, also with a lower density, the intergranular distances in CN microstructures are more likely to increase with the temperature gradient. Nevertheless, these results show a high homogeneity of the characteristics of this bio-material. and describe a linear decreasing trend of the calculated parameters: young modulus, hardness, creep coefficient and toughness.

The mechanical results show that the CN and CS materials are very hard and tough comparing to wood product.

Indentation analyses showed two distinct regimes, which are an elastic regime and a plastic regime with strain-hardening. The elastic phase was reduced with increasing temperature ranges. The elastic behaviour is similar to the friction of the microparticles during penetration and when the temperature increases, the intergranular bonding energy will become insufficient to the indentation energies to avoid microcracking, indicating the end of the plastic phase. Plastic behaviour can be understood as a combination of energy absorption mechanisms, including cell crushing, intergranular bond failure, primary wall failure and cell tearing. When the sample densifies by crushing the porosities, the dissipation of frictional energy is greater because the elastic capacity of the materials is almost completely lost.

It is noted that from an isothermal temperature of 70 °C, the mechanical properties are strongly influenced, this due to the approach of the glass transition zone. This is confirmed by a reduction in modulus of elasticity, hardness and toughness by half for CS and almost a quarter for CN.

Figure 8 shows an Ashby graph for compressive strength (calculated by its relationship to hardness) as a function of density and compressive strength for different materials. CN and CS materials show higher

Table 2. Summary of characterization data for CN and CS and some similar materials.

Nature of samples	Temp/°C	Density Kg/m^3 (s.d.)	Hardness/MPa (s.d.)	Reduced young's moduls/GPa (s.d.)	Creep coefficient/Value (s.d.)	Toughness/MPa.m$^{-0.5}$ (s.d.)	Strength MPa (s.d.)
Cocos nucifera (**current study**)	30	1.49 (0.22)	135.26 (8.11)	4.63 (0.41)	23 (1.38)	6.07 (0.30)	49.95 (4.30)
	50	/	115.71 (5.78)	2.78 (0.25)	23.44 (1.40)	3.65 (0.18)	35.34 (3.12)
	70	/	97.02 (7.76)	1.89 (0.17)	25 (1.5)	3.13 (0.15)	33.34 (7.75)
	90	/	85.79 (3.43)	1.68 (0.15)	32.43 (1.94)	2.36 (0.11)	26.56 (0.30)
Canarium schweinfurthii (**current study**)	30	1.46 (0.21)	136.48 (13.64)	4.61 (0.46)	26 (2.86)	6 (0.42)	49.50 (0.30)
	50	/	96.57 (9.65)	4.26 (0.42)	26.09 (2.86)	4.91 (0.34)	42.35 (0.30)
	70	/	91.11 (9.11)	4.18 (0.41)	28.46 (3.13)	4.02 (0.28)	35.51 (0.30)
	90	/	72.56 (7.25)	2.62 (0.26)	28.71 (3.15)	3.14 (0.21)	31.40 (0.30)
Elaeis guineensis (oil palm)	30	1.14[a]	126.3 (20.6)[b]	2.46 (1.04)[b]	/	/	12.06 (1.98)[a]
Acrocomia Mexicana (cocoyol) [3]	30	1.25 (0.03)	290 (25)	9.1 (1.28)	/	/	87.3 (12.2)
Macadamia ternifolia	30	1.27[c]	180 (30)[c]	84 (9)[c]		1.13 (0.12)[d]	84.3 (9)[d]
Scheelea sp.	30		271.5 (74.7)[b]	3.80 (0.99)[b]		2.77 (1.11)[e]	
Hazelnut	30	1.05[f]	7.18[e]	0.194[e]			
Brazil nut	30		7.13[e]	0.198[e]			

[5] [68].
[6] [3].
[7] [67].
[8] [69].
[9] [70].
[10] [71].

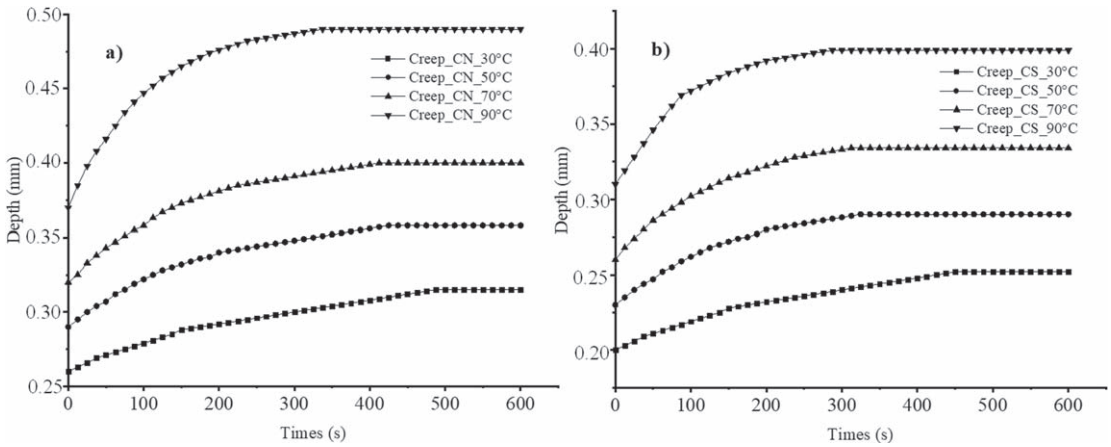

Figure 7. Creep curve function of temperature, (a) CN material; (b) CS material.

Table 3. Summary of creep parameters.

		CN				CS			
	Unit	30 °C	50 °C	70 °C	90 °C	30 °C	50 °C	70 °C	90 °C
ε_0	mm	0.26	0.29	0.32	0.37	0.20	0.23	0.26	0.31
ε_t	mm	0.31	0.36	0.40	0.49	0.25	0.29	0.33	0.40
ε_0^{fl}	mm	0.29	0.33	0.37	0.44	0.23	0.27	0.30	0.36
ε_{ip}	mm	0.28	0.32	0.37	0.47	0.21	0.26	0.31	0.38
$\dot{\varepsilon}_t$ ($\times 10^{-5}$)	mm s^{-1}	9.17	11.33	13.33	20.00	8.67	10.00	12.33	14.83
$\dot{\varepsilon}_p$ ($\times 10^{-5}$)	mm s^{-1}	11.60	8.24	7.53	5.05	8.00	8.00	8.32	7.00
D_0 ($\times 10^{-3}$)	MPa^{-1}.mm	1.79	2.86	3.46	4.58	1.38	1.82	2.31	3.25
g_0		1.21	1.23	1.25	1.32	1.26	1.27	1.28	1.29

performance compared to other biological materials such as wood. Their properties allow them to be classified in the range of synthetic materials used as structural fillers in the development of composites.

A comparison of the mechanical properties of various fruits and stone shells is presented in table 2. Since most of the data available for these types of shells come from indentation tests, only Er and H values are presented for all these shells. It is found that the CN and CS core shells have similar mechanical properties to the other shells.

4. Conclusion

In this study, the mechanical characteristics and rheological behaviour of certain by-products of cameroonian plants (CN and CS) were experimentally determined at different isotherms by macroindentation. Using a spherical indenter of Φ6mm and for loads up to 500N, several tests were carried out on both materials at isotherms of 30 °C, 50 °C, 70 °C and 90 °C. The Oliver and Pharr method exploited in macroindentation made it possible to determine the reduced Young's modulus, hardness, creep coefficient, toughness, mechanical strength and rheological model of these biomaterials. The results show that, apart from the creep coefficient, all other characteristics decrease with temperature in the mentioned range. Temperature has a great influence on parameters such as Young's modulus (its value drops by about 50% between 30 °C and 90 °C) and toughness (its value drops by about 60% between 30 °C and 90 °C). Overall, the mechanical characteristics of CN are more sensitive to temperature than those of CS. Conversely, the creep coefficient increases slightly with temperature. Of the four rheological models tested, the Burger-4 elements model best reflects the behavior of CN and CS. All its results show that CN and CS can be used as reinforcing elements in composite materials. This study also made it possible to classify CN and CS according to an Ashby diagram in the engineer's polymer category.

Table 4. Simulated rheological models parameters.

Models			$\frac{\sigma}{E_0}$	$\frac{\sigma}{\eta_0}$ x 10^{-5}	$\frac{\sigma}{E_1}$	$\frac{1}{\tau_1}$	R^2
Newton	CN	30 °C	0.27	8.81			0.939
		50 °C	0.31	9.85			0.832
		70 °C	0.35	11.22			0.793
		90 °C	0.43	13.81			0.643
	CS	30 °C	0.21	8.29			0.913
		50 °C	0.25	8.03			0.718
		70 °C	0.29	9.38			0.692
		90 °C	0.357	9.74			0.582
Kelvin	CN	30 °C			0.30	6.74	−5.11
		50 °C			0.35	0.42	−4.567
		70 °C			0.39	8.21	−3.85
		90 °C			0.48	10.02	−2.516
	CS	30 °C			0.24	7.97	−3.203
		50 °C			0.28	0.19	−3.676
		70 °C			0.32	0.23	−3.277
		90 °C			0.39	9.49	−3.323
Zener	CN	30 °C	0.26		0.06	318.70	0.995
		50 °C	0.23		0.07	171.80	0.997
		70 °C	0.32		0.08	150.00	0.998
		90 °C	0.37		0.12	98.17	0.998
	CS	30 °C	0.21		0.05	263.40	0.995
		50 °C	0.23		0.06	125.30	0.994
		70 °C	0.26		0.07	116.40	0.994
		90 °C	0.31		0.09	84.57	0.997
Burger 4	CN	30 °C	0.26	1.04	0.05	280.60	0.995
		50 °C	0.29	−1.28	0.08	193.90	0.997
		70 °C	0.32	−2.24	0.09	179.00	0.998
		90 °C	0.37	−1.91	0.13	110.30	0.999
	CS	30 °C	0.20	−10.15	0.17	585.80	0.996
		50 °C	0.23	−3.88	0.08	180.50	0.998
		70 °C	0.26	−3.83	0.09	159.30	0.998
		90 °C	0.31	−1.27	0.09	93.95	0.998

Table 5. Calculation of Burger-4 elements model parameters.

Samples	T (°C)	σ (MPa)	E_0 (MPa)	E_1 (MPa)	η_0 (MPa.s)	τ_1 (s)
CN	30 °C	144.68	554.35	2562.63	138.98×10^5	21.38×10^{-2}
	50 °C	101.44	349.21	1273.45	79.19×10^5	30.94×10^{-2}
	70 °C	92.44	288.89	951.38	41.32×10^5	33.51×10^{-2}
	90 °C	80.71	217.71	617.94	42.41×10^5	54.39×10^{-2}
CS	30 °C	144.68	718.41	823.95	14.25×10^5	10.24×10^{-2}
	50 °C	126.50	551.46	1472.69	32.61×10^5	33.24×10^{-2}
	70 °C	112.52	431.79	1155.99	29.41×10^5	37.66×10^{-2}
	90 °C	95.25	309.96	965.15	75.23×10^5	63.86×10^{-2}

Acknowledgments

The authors would like to thank the participation of Armel Waffo Fogue, Adonis Mounchigam Mfouapon, Syrille Bryce Tchinwoussi and Jonathan Sesyi for their participation during the Lab's activities.

Compliance with ethical standards

Conflict of interest: The authors declare that they have no competing interests.

Conflict of interest

The authors declare that they have no competing interests.

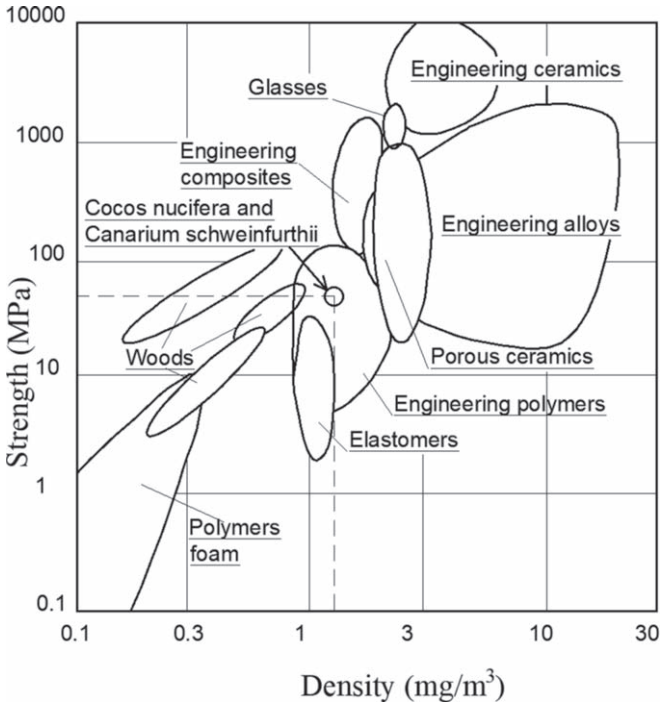

Figure 8 Classification of CN and CS materials in an Ashby diagram.

ORCID iDs

Bernard Morino Ganou Koungang https://orcid.org/0000-0002-2630-4999
Dieunedort Ndapeu https://orcid.org/0000-0003-0793-9785
Jerôme Tchoufang Tchuindjang https://orcid.org/0000-0002-4688-6092
Gilbert Tchemou https://orcid.org/0000-0003-4231-289X
Ebénézer Njeugna https://orcid.org/0000-0002-3475-034X
Luc Courard https://orcid.org/0000-0001-6573-6631

References

[1] Vinod A, Sanjay M R, Siengchin S and Jyotishkumar P 2020 Renewable and sustainable biobased materials: an assessment on biofibers, biofilms, biopolymers and biocomposites *J. Clean. Prod.* **258** 120978
[2] Alharbi M A H, Hirai S, Tuan H A, Akioka S and Shoji W 2020 Effects of chemical composition, mild alkaline pretreatment and particle size on mechanical, thermal, and structural properties of binderless lignocellulosic biopolymers prepared by hot-pressing raw microfibrillated Phoenix dactylifera and Cocos nucifera *Polym. Test.* **84** 106384
[3] Flores-Johnson E A, Carrillo J G, Zhai C, Gamboa R A, Gan Y and Shen L 2018 Microstructure and mechanical properties of hard Acrocomia mexicana fruit shell *Sci. Rep.* **8** 1–12
[4] Dirisu J O, Fayomi O S I, Oyedepo S O and Akinlabi E T 2019 A preliminary study on chemical and physical properties of coconut shell powder as an enhancer in building ceilings for construction industry: a mini review *IOP Conf. Ser.: Mater. Sci. Eng.* **640** 12063
[5] Nadzri S N I H A *et al* 2020 A comprehensive review of coconut shell powder composites: preparation, processing, and characterization *J. Thermoplast. Compos. Mater.* **In press** 1–240892705720930808
[6] Senthilkumar K, Chandrasekar M, Rajini N, Siengchin S and Rajulu V 2019 Characterization, thermal and dynamic mechanical properties of poly(propylene carbonate) lignocellulosic Cocos nucifera shell particulate biocomposites *Mater. Res. Express* **6** 96426
[7] Mittal M and Chaudhary R 2019 Biodegradability and mechanical properties of pineapple leaf/coir Fiber reinforced hybrid epoxy composites *Mater. Res. Express* **6** 45301
[8] Jaya prithika A and Sekar S K 2016 Mechanical and fracture characteristics of Eco-friendly concrete produced using coconut shell, ground granulated blast furnace slag and manufactured sand *Constr. Build. Mater.* **103** 1–7
[9] Lecompte T, Perrot A, Subrianto A, Le Duigou A and Ausias G 2015 A novel pull-out device used to study the influence of pressure during processing of cement-based material reinforced with coir *Constr. Build. Mater.* **78** 224–33
[10] Ali M, Liu A, Sou H and Chouw N 2012 Mechanical and dynamic properties of coconut fibre reinforced concrete *Constr. Build. Mater.* **30** 814–25
[11] Mittal M and Chaudhary R 2018 Experimental investigation on the mechanical properties and water absorption behavior of randomly oriented short pineapple/coir fiber-reinforced hybrid epoxy composites *Mater. Res. Express* **6** 15313
[12] Faria D L *et al* 2020 Physical and mechanical properties of polyurethane thermoset matrices reinforced with green coconut fibres *J. Compos. Mater.* **In press** 1–120021998320940023
[13] Srivaro S, Tomad J, Shi J and Cai J 2020 Characterization of coconut (Cocos nucifera) trunk's properties and evaluation of its suitability to be used as raw material for cross laminated timber production *Constr. Build. Mater.* **254** 119291

[14] Lai C Y, Sapuan S M, Ahmad M, Yahya N and Dahlan K Z H M 2005 Mechanical and electrical properties of coconut coir fiber-reinforced polypropylene composites *Polym. Plast. Technol. Eng.* **44** 619–32

[15] Robert U W, Etuk S E, Umoren G P and Agbasi O E 2019 Assessment of thermal and mechanical properties of composite board produced from coconut (cocos nucifera) husks, waste newspapers, and cassava starch *Int. J. Thermophys.* **40** 83

[16] Naveen J, Jawaid M, Zainudin E, Sultan M and Yahaya R 2019 Enhanced thermal and dynamic mechanical properties of synthetic/natural hybrid composites with graphene nanoplateletes *Polymers (Basel).* **11** 1085

[17] Naveen J, Jawaid M, Zainudin E S, Sultan M and Yahaya R 2019 Mechanical and moisture diffusion behaviour of hybrid Kevlar/Cocos nucifera sheath reinforced epoxy composites *J. Mater. Res. Technol.* **8** 1308–18

[18] Marceau S, Caré S and Lesage P 2016 Synthèse de l'opération de recherche stratégique et incitative *Matériaux Biosourcés Et Naturels Pour Une Construction Durable* (Mabionat)

[19] Lagel M-C 2015 *Développement de Nouveaux Matériaux à Base de Polymères Naturels et Leurs Applications* (Lorraine: Université de Lorraine)

[20] Winters R F 1969 *Newer Engineering Materials: A Symposium on Recent Developments in New Materials for Use in Engineering* (London: MacMillan)

[21] Callister W D and Rethwisch D G 2011 *Materials Science and Engineering* 5th edn (New York: wiley)

[22] Murr L E 2015 *Handbook of Materials Structures, Properties, Processing and Performance* (Switzerland: Springer)

[23] Hiloidhari M *et al* 2020 *Agroindustry Wastes: Biofuels and Biomaterials Feedstocks for Sustainable Rural Development, In Refining Biomass Residues for Sustainable Energy and Bioproducts* (Amsterdam: Elsevier) 357–88

[24] Gogoi D 2014 *Valorization of Bio-Waste for Biofuel and Biomaterials* (Tezpur: Tezpur University)

[25] Bontempi E 2017 *A new Approach to Evaluate the Sustainability of Raw Materials Substitution, In Raw Materials Substitution Sustainability* (Berlin: Springer) 79–101

[26] Henstock M E 1988 The impacts of materials substitution on the recyclability of automobiles *Resour. Conserv. Recycl.* **2** 69–85

[27] Chen M, Blanc D, Gautier M, Mehu J and Gourdon R 2013 Environmental and technical assessments of the potential utilization of sewage sludge ashes (SSAs) as secondary raw materials in construction *Waste Manag.* **33** 1268–75

[28] CIRAD 2006 *Annual Report CIRAD 2006: Growing Crops in Town A Response to Urbanization* (Paris: CIRAD)

[29] Ndapeu D *et al* 2020 Elaboration and characterization of a composite material based on canarium schweinfurthii engl cores with a polyester matrix *Mater. Sci. Appl.* **11** 204–15

[30] Fathi L and Frühwald A 2014 The role of vascular bundles on the mechanical properties of coconut palm wood *Wood Mater. Sci. Eng.* **9** 214–23

[31] Rana M N, Das A K and Ashaduzzaman M 2015 Physical and mechanical properties of coconut palm (Cocos nucifera) stem *Bangladesh J. Sci. Ind. Res.* **50** 39–46

[32] Niklas K J and Spatz H-C 2010 Worldwide correlations of mechanical properties and green wood density *Am. J. Bot.* **97** 1587–94

[33] Monteiro S N, Terrones L A H and D'Almeida J R M 2008 Mechanical performance of coir fiber/polyester composites *Polym. Test.* **27** 591–5

[34] Rahman M M and Khan M A 2007 Surface treatment of coir (Cocos nucifera) fibers and its influence on the fibers' physico-mechanical properties *Compos. Sci. Technol.* **67** 2369–76

[35] Ze E P *et al* 2020 Elaboration and characterization of composite materials reinforced by papaya trunk fibers (carica papaya) and particles of the hulls of the kernels of the winged fruits (canarium schweinfurthii) with polyester matrix *J. Miner. Mater. Charact. Eng.* **08** 341–52

[36] Srinivasababu N 2017 Mechanical behavior of arbitrarily reinforced cocos nucifera leaf sheath fibre reinforced polyester composites—comparison with other coconut FRP composites *Mater. Today Proc.* **4** 9612–5

[37] Apasi A, Yawas D S, Abdulkareem S and Kolawole M Y 2016 Improving mechanical properties of aluminium alloy through addition of coconut shell-ash *J. Sci. Technol.* **36** 34–43

[38] Gludovatz B, Walsh F, Zimmermann E A, Naleway S E, Ritchie R O and Kruzic J J 2017 Multiscale structure and damage tolerance of coconut shells *J. Mech. Behav. Biomed. Mater.* **76** 76–84

[39] Ndapeu D, Demze Nitidem A, Sikame Tagne N R, Ganou Koungang B M, Defo N and Njeugna E 2020 Characterization of a brake lining composite based on aiele fruit cores (Canarium schweinfurthii) and palm kernel fibers (elaeis guineensis) with a urea-formaldehyde matrix *Int. J. Sci. Eng. Res.* **11** 1110–7 http://www.ijser.org/onlineResearchPaperViewer.aspx?CHARACTERIZATION-OF-A-BRAKE-LINING-COMPOSITE-BASED-ON-AIELE-FRUIT-CORES-CANARIUM-SCHWEINFURTHII-AND-PALM-KERNEL-FIBERS.pdf

[40] Ehiem J C, Ndirika V I O, Onwuka U N and Raghavan V 2019 The moisture-dependent flow characteristics of canarium schweinfurthii engler nuts *Res. Agric. Eng.* **65** 40–7

[41] Schmier S, Hosoda N and Speck T 2020 Hierarchical structure of the cocos nucifera (coconut) endocarp: functional morphology and its influence on fracture toughness *Molecules* **25** 223

[42] Shen J, Flores M and Sharits A 2020 Impact performance of a plate structure with coconut-inspired microchannels *Appl. Sci.* **10** 355

[43] Vidil L, Potiron C O, Bilba K and Arsène M-A 2020 Characterization of a new native plant textile, leaf sheath from cocos nucifera l., as potential reinforcement of polymer composites *Ann. Agric. Crop Sci.* **5** 1056

[44] Brebbia C A and Klemm A 2013 *Materials Characterisation VI: Computational Methods and Experiments* 77 (Ashurst: WIT Press) 364

[45] Flewitt P E J and Wild R K 2017 *Physical Methods for Materials Characterisation* (Boca Raton, FL: CRC Press)

[46] Sakai M 2008 Principles and applications of indentation *micro and nano mechanical testing of materials and devices* ed F Yang and J C M Li (Switzerland: Springer Science+Business Media, LLC) 1–47

[47] Ganou Koungang B M, Ndapeu D, Tchemou G, Njeugna E and Courard L 2019 Comportement Hydromécanique des BTC Avec Granulats de Canarium Schweinfurthii et Cocos Nucifera: Analyse de Durabilité *Colloque International des 4Oaires de l'Enset de Douala (Douala, 04-12-2019 to 07-12-2019)* (Marseille: Raiffet) 10 http://hdl.handle.net/2268/243539

[48] William D G R, Callister D Jr, William J, Callister D and Rethwisch D G 2010 Materials science and engineering *An Introduction, Mater. Sci. Eng. an Introd.* **1** 885

[49] Njeugna E, Ganou M B K, Ndapeu D, Foba J N T, Sikame N R T and Huisken P W M 2016 An instrumented macro-indentation method for determining the mechanical properties of coconut shell (coco nucifera of cameroon) *Mech. Mater. Sci. Eng. J.* **5** 8 https://hal.archives-ouvertes.fr/hal-01367491

[50] Dos Reis J M L 2012 Effect of temperature on the mechanical properties of polymer mortars *Mater. Res.* **15** 645–9

[51] Plaseied A and Fatemi A 2008 Strain rate and temperature effects on tensile properties and their representation in deformation modeling of vinyl ester polymer *Int. J. Polym. Mater. Polym. Biomater.* **57** 463–79

[52] Njeugna E, Ndapeu D, Bistac S, Foba J and Fogue M 2013 Contribution to the characterisation of the coconut shells (coco nucifera) of cameroon *Int. J. Mech. Struct.* **4** 1–22 http://www.irphouse.com/ijms/ijmsv4n1_01.pdf
[53] Oliver W and Pharr G M 1992 An improved technique for determining hardness and elastic modulus using load and displacement sensing indentation experiments *J. Mater. Res.* **7** 1564–83
[54] Chudoba T and Jennett N M 2008 Higher accuracy analysis of instrumented indentation data obtained with pointed indenters *J. Phys. D: Appl. Phys.* **41** 215407
[55] Oliver W and Pharr G M 2004 Measurement of hardness and elastic modulus by instrumented indentation: advances in understanding and refinements to methodology *J. Mater. Res.* **19** 3–20
[56] Herbert E G, Pharr G M, Oliver W C, Lucas B N and Hay J L 2001 On the measurement of stress-strain curves by spherical indentation *Thin Solid Films* **398–399** 331–5
[57] Sun M C, Yang C, Xiao S Y, Tan W and Zhou G P 2019 Analysis of the mechanical properties of Q345R steel in deep-regulating units by the spherical indentation method *IOP Conf. Ser.: Mater. Sci. Eng.* **668** 012017
[58] Arizzi F and Rizzi E 2014 Elastoplastic parameter identification by simulation of static and dynamic indentation tests *Model. Simul. Mater. Sci. Eng.* **22** 035017
[59] Celentano D J, Guelorget B, François M, Cruchaga M A and Slimane A 2012 Numerical simulation and experimental validation of the microindentation test applied to bulk elastoplastic materials *Model. Simul. Mater. Sci. Eng.* **20** 045007
[60] Yoffe E H 1984 Modified Hertz theory for spherical indentation *Philos. Mag. A Phys. Condens. Matter, Struct. Defects Mech. Prop.* **50** 813–28
[61] Oliver W C and Pharr G M 1992 An improved technique for determining hardness and elastic modulus using load and displacement sensing indentation experiments *J. Mater. Res.* **7** 1564–83
[62] Schapery R A 1964 Effect of cyclic loading on the temperature in viscoelastic media with variable properties *AIAA J.* **2** 827–35
[63] Schapery R A 1966 A theory of non-linear thermoviscoelasticity based on irreversible thermodynamics *5th U.S. Congress of Applied Mechanics* 511–30
[64] Sikame Tagne N R *et al* 2018 Study of the viscoelastic behaviour of the Raffia vinifera fibres *Ind. Crops Prod.* **124** 572–81
[65] Chai H and Lawn B R 2007 A universal relation for edge chipping from sharp contacts in brittle materials: a simple means of toughness evaluation *Acta Mater.* **55** 2555–61
[66] Hills D A, Nowell D and Barber J R 2017 KL Johnson and contact mechanics *Proc. Inst. Mech. Eng. Part C J. Mech. Eng. Sci.* **231** 2451–8
[67] Kaupp G and Naimi-Jamal M R 2011 Nutshells' mechanical response: From nanoindentation and structure to bionics models *J. Mater. Chem.* **21** 8389–90
[68] Okpala D C 1990 Palm kernel shell as a lightweight aggregate in concrete *Build. Environ.* **25** 291–6
[69] Wang C-H and Mai Y-W 1994 Deformation and fracture of Macadamia nuts *Int. J. Fract.* **69** 67–85
[70] Lucas P W *et al* 2009 Indentation as a technique to assess the mechanical properties of fallback foods *Am. J. Phys. Anthropol.* **140** 643–52
[71] Maleki G, Milani J and Motamedzadegan A 2013 Some physical properties of azarbayejani hazelnut and its kernel *Int. J. Food Eng.* **9** 135–40